Progress In Electromagnetics Research M, Vol. 106, 179–189, 2021

Synthesis of Wideband Reconfigurable Array Antennas for Monopulse Radar Applications

Le T. P. Bui[3], Nicola Anselmi[3], Giada M. Battaglia[1, 2], Tommaso Isernia[1, 2], Paolo Rocca[3, 4], and Andrea F. Morabito[1, 2, *]

Abstract—A new approach to the bandwidth maximization of reconfigurable antenna arrays for monopulse radar applications is proposed and tested. The provided radiating systems allow switching the radiation behavior from sum to difference patterns (and vice versa) while sharing the excitation amplitudes of a user-decided set of radiating elements. Furthermore, the proposed design procedure guarantees the maximum possible bandwidth performance once the overall antenna size, the desired beamwidth, sidelobe level, and slope in the target direction of the generated power patterns are fixed. The synthesis problem is cast and solved as a sequence of convex programming optimizations, and hence the maximization of performances is attained with advantages in terms of computational times as well as convergence to the global optimum. The given theory is supported by numerical experiments including arrays with ultra-wideband performances.

1. INTRODUCTION

Monopulse array antennas, conceived as systems respectively operating through sum and difference patterns in the transmission and reception modalities, represent one of the most common (yet important) solutions in order to significantly increase any radar accuracy [1–8].

In the design of this kind of antennas, for fixed beamwidth performances and array geometries, one is usually interested in finding the array excitations in such a way to achieve the 'optimal compromise' [4] between the sum pattern's beamwidth and the difference pattern's slope in the target direction, while the sidelobe level (SLL) is kept as low as possible in both radiation modalities and in particular in the sum pattern.

Several approaches aimed at optimally solving this design problem have been proposed in the last years, often relying on computationally expensive global-optimization strategies (see for instance [5]) or subarraying techniques [6]. A much more effective approach, based exclusively on Convex Programming (CP) and hence guaranteeing the achievement of the (unique) globally-optimal solution of the problem as well as the minimization of the corresponding computational time, has been proposed by the authors in [7] and [8] for linear and planar monopulse arrays, respectively. Notably, the approach also allows switching between the sum and difference patterns by acting on the excitation amplitude of a small portion of the radiating elements (which is a-priori identified by the user — see Fig. 1). In this way, the user can a-priori restrict or minimize the number of amplifiers required for the beam forming network (BFN) and hence reduce the hardware complexity and costs.

The main limitation affecting the approaches recalled above and essentially all the techniques devoted to the synthesis of monopulse arrays is the single-frequency or the narrow-band assumption.

Received 9 September 2021, Accepted 8 December 2021, Scheduled 24 December 2021

* Corresponding author: Andrea Francesco Morabito (andrea.morabito@unirc.it).

[1] Department of Information Engineering, Infrastructures, and Sustainable Energy, Università di Reggio Calabria, Reggio Calabria 89122, Italy. [2] CNIT (Consorzio Nazionale Interuniversitario per le Telecomunicazioni), Parma 43124, Italy. [3] ELEDIA Research Center (ELEDIA@UniTN — Università di Trento), via Sommarive, Trento I-38123, Italy. [4] ELEDIA Research Center (ELEDIA@XIDIAN — Xidian University), P. O. Box 191, No. 2 South Tabai Road, Xi'an, Shaanxi Province 710071, China.

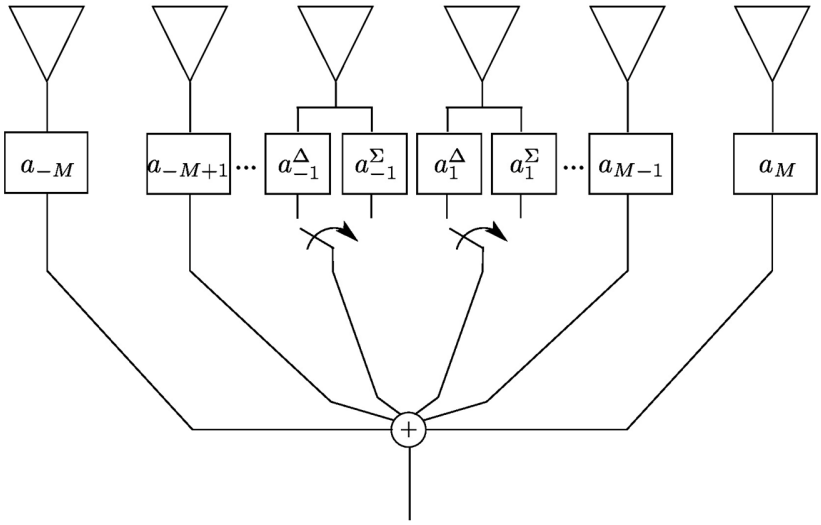

Figure 1. Sketch of the reconfigurable array architecture switching from the sum to the difference patterns where $a^{\Sigma}_{-M}, \ldots, a^{\Sigma}_{M}$ and $a^{\Delta}_{-M}, \ldots, a^{\Delta}_{M}$ respectively denote the complex excitations corresponding to the two radiation modalities. In the depicted instance, the reconfiguration is performed by just changing the amplitude and phase of the two central coefficients (while all the remaining excitations must not be changed in order to switch from the sum to the difference pattern).

In particular, the optimal compromise among sum and difference patterns is systematically pursued by fixing once and for all the working frequency to a single prescribed value [1–8]. This is also the case where the synthesis of a single pencil [9–12] or shaped [13–15] beam is addressed.

Obviously, while the synthesis algorithms are simplfied, the single-frequency assumption restricts the application range of the designed antennas. In fact, with respect to wideband devices, narrowband systems exhibit several disadvantages including, just to cite a few, higher electromagnetic radiation and energy consumption as well as a lower precision in range. As a matter of fact, the capability of a radiating system to guarantee wideband performances has become essential in most applications of actual interest including, just to cite a few, MIMO telecommunications, 5G smartphone transmissions, and WiMAX & WLAN applications [16–21].

To contribute to address this issue, the authors recently developed in [21] an innovative approach to the synthesis of pencil-beam arrays granting the maximum possible bandwidth. In particular, the approach in [21] extended the seminal technique published in [22] for the SLL optimization to the case where the radiation performance has to be guaranteed over the largest possible frequency range.

In so doing, the maximization of radiation performances provided by [22] has been kept by casting the problem as a sequence of CP optimizations. Notably, as the bandwidth maximization is performed just in the case where the array must generate a single sum pattern, it remains an open challenge in the case of monopulse antennas simultaneously generating sum and difference beams.

By taking into account all the above, this contribution proposes a new approach definitively unifying the techniques introduced in [7] and [21] in order to perform the synthesis of wideband monopulse arrays. In particular, the new technique jointly exploits the method developed in [7] (in order to perform the optimal synthesis of sum and difference patterns with arbitrary sidelobes subject to common excitations constraints) and the strategy introduced in [21] (in order to maximize the bandwidth of fixed-geometry arrays). As a consequence, the synthesized arrays are able to reconfigure their radiation behavior from the sum pattern to the difference pattern (and vice versa) over the largest possible frequency range, leading to a wideband monopulse system. As a distinguishing feature, the new technique relies only on CP optimizations and hence keeps the effectiveness and reliability of its predecessors.

In the following, the design procedure is presented in Section 2 while numerical examples including ultra-wideband (UWB) monopulse arrays are given in Section 3. Conclusions follow (Section 4).

2. THE PROPOSED APPROACH

The proposed approach can be applied to any fixed-geometry linear or planar array, whatever the elements' location and radiation pattern, provided that the layout exhibits any symmetry allowing the phase-only reconfiguration between sum and difference patterns (see [7, 8] for more details). However, in order to simplify its presentation, in the following the synthesis problem is cast for the case of linear equispaced arrays whose far field pattern can be expressed in terms of the array factor. To this end, let us consider the array geometry depicted in Fig. 2, i.e., a 1-D array composed by $N = 2M$ radiating elements symmetrically located on the z-axis, and let us express the corresponding radiation pattern as:

$$AF(f,\theta) = \sum_{\substack{m=-M \\ m\neq 0}}^{M} a_m e^{j\frac{2\pi f}{c} z_m \cos\theta} \tag{1}$$

where for $m = -M, \ldots, M$, $a_m = |a_m| \exp(j\varphi_m)$ and z_m respectively represent the complex excitation and the location of the m-th element; θ is the observation angle from the z-axis; f is the operating frequency; and c is the speed of light in vacuum.

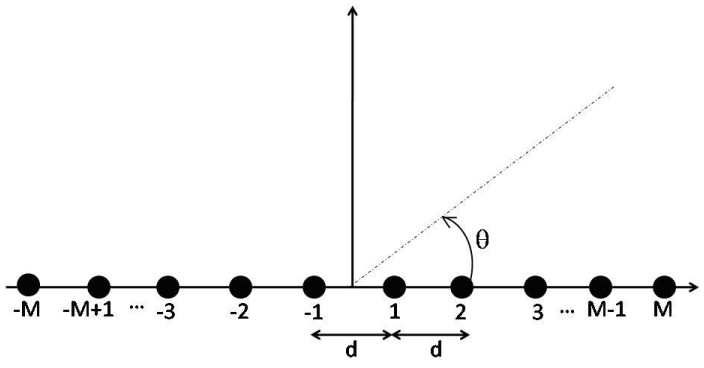

Figure 2. Sketch of the array geometry.

Once the array elements' number and locations have been fixed, the goal is to identify two sets of excitations, namely $a^{\Sigma}_{-M}, \ldots, a^{\Sigma}_{M}$ and $a^{\Delta}_{-M}, \ldots, a^{\Delta}_{M}$, respectively generating the reconfigurable sum and difference patterns, say AF^{Σ} and AF^{Δ}, over the largest possible frequency range. Moreover, in order to simplify the monopulse reconfiguration, the amplitude of the two excitation sets must be shared between the two radiation modalities over a portion of the layout chosen by the user according to the desired performance and the particular scenario at hand.

To present the approach, let us denote with $f_{\max}$ the maximum operating frequency of the array and, as in [21], and consider a discrete set of frequencies $f_1, \ldots, f_Q$ such that $f_1 = f_{\max}$ and $f_q = f_{\max} - (q-1)\Delta f$, $q = 2, \ldots, Q$. Therefore, Δf and $f_{\min} = f_{\max} - (Q-1)\Delta f$ respectively denote the difference between two consecutive frequencies and the minimum operating frequency of the array. Then, by denoting with Ω_{Σ} and Ω_{Δ} the sidelobes' regions respectively pertaining to the sum and difference radiation modalities, let us suppose that one aims at enforcing, inside them, arbitrary upper-bound constraints through the real and positive functions UB_{Σ} and UB_{Δ}, respectively. Finally, by denoting with θ_T the target direction, the synthesis problem at hand can be cast as the identification of the array excitations as follows:

$$\max_{a^{\Sigma}_1,\ldots,a^{\Sigma}_M,a^{\Delta}_1,\ldots,a^{\Delta}_M} Q \tag{2}$$

$$subject\ to:$$

$$\begin{cases} AF^{\Sigma}(f_q,\theta)\big|_{\theta=\theta_T} = A_{\Sigma} & q=1,\ldots,Q & & (3a)\\ \dfrac{\partial AF^{\Delta}(f_q,\theta)}{\partial\theta}\Big|_{\theta=\theta_T} = A_{\Delta} & q=1,\ldots,Q & & (3b)\\ \left|AF^{\Sigma}(f_q,\theta)\right|^2 \le UB_{\Sigma}(\theta) & q=1,\ldots,Q & \forall\theta\in\Omega_{\Sigma} & (3c)\\ \left|AF^{\Delta}(f_q,\theta)\right|^2 \le UB_{\Delta}(\theta) & q=1,\ldots,Q & \forall\theta\in\Omega_{\Delta} & (3d)\\ a_m^{\Sigma} = a_m^{\Delta} & m=N_C,\ldots,M & N_C\ge 1 & (3e)\\ a_{-m}^{\Sigma} = a_m^{\Sigma} & m=1,\ldots,M & & (3f)\\ a_{-m}^{\Delta} = -a_m^{\Delta} & m=1,\ldots,M & & (3g) \end{cases}$$

where A_{Σ} and A_{Δ} are real and positive coefficients chosen by the user according to the particular requirements at hand, while the observation variable θ is meant to be discretized by following the rules in [23].

In the above optimization problem, for any frequency belonging to set $f_1,\ldots,f_Q$, constraints (3a) and (3c) allow generating the sum pattern with a prescribed SLL and beamwidth while constraints (3b) and (3d) grant the desired slope in the target direction and SLL performance for the difference pattern. Furthermore, due to the array layout symmetry, constraints (3f) and (3g) ensure that the sum and difference patterns respectively result in an even function and an odd function of θ which, in turn, is essential in order to guarantee that AF^{Δ} is equal to zero at boresight whatever the working frequency is. Moreover, these two sets of constraints entail that the sum and difference power patterns are even functions and hence that the SLL can be kept under control by enforcing the upper-bound masks only for $\theta=[0,\pi/2]$ with a consequent reduction of the computational time. Finally, constraints (3e) are aimed at simplifying the reconfiguration from the sum pattern to the difference pattern (and vice versa). In fact, switching between the two radiation modalities will require acting on both the amplitude and phase of only $2(N_C-1)$ excitations while the remaining $2(M-N_C+1)$ excitations will be subject to a change only in terms of phase. In particular, the amplitude of the $2(M-N_C+1)$ elements located on the outer part of the array layout will be shared between the two radiation modalities. Such a choice, which is suggested by the 'common tail' behavior of the ideal current distributions pertaining to the sum and difference patterns (see [7] for more details), allows a significant reduction of the BFN complexity.

The most convenient reconfiguration scheme will be achieved for $N_C=1$ which leads to a phase-only reconfigurable array (i.e., $|a_m^{\Sigma}|=|a_m^{\Delta}|$ for $m=1,\ldots,M$) and hence to the minimum possible complexity of the feeding network. On the other hand, the lower the N_C is, the lower the expected radiation performance of the two reconfigurable patterns is. In any case, the extremely-low required computational time (see below) allows the user to readily find the best (desired) compromise between the maximization of radiation performances and the minimization of the hardware cost and complexity.

While fulfilling constraints (3) guarantees all the interesting features described above, maximization (2) allows maximizing the width of the frequency range on which they are actually realized. In particular, since the fractional bandwidth (FBW) [24–26] is defined as:

$$FBW = 2\frac{f_{\max}-f_{\min}}{f_{\max}+f_{\min}} \tag{4}$$

the synthesized array will guarantee the following bandwidth performance:

$$FBW = 2\frac{Q-1}{\dfrac{2f_{\max}}{\Delta f}-Q+1} = \frac{W}{\dfrac{f_{\max}}{\Delta f}-\left(\dfrac{W}{2}\right)} \qquad with \qquad W=Q-1 \tag{5}$$

While $f_{\max}$ and Δf can be chosen according to rules analogous to the ones listed in in [21] (note that strategies to optimally select the array inter-element spacing and avoid superdirective sources can also be applied), it is worth noting that the array will result in 'wideband' (i.e., $0.2<FBW<0.5$) as long as $2.5<(f_{\max}/W\Delta f)<5.5$ and 'ultra-wideband' (i.e., $FBW\ge 0.5$) as long as $(f_{\max}/W\Delta f)\le 2.5$.

Notably, once a sufficiently-fine discretization is performed by exploiting the bandlimitedness of AF^{Σ} and AF^{Δ} [23], the constraints (3a), (3b), (3e), (3f), (3g) and the constraints (3c), (3d) result in, respectively, linear and positive semidefinite quadratic forms of the unknowns. Therefore, (3) is a

system of *linear* equalities and *quadratic* inequalities in the array excitations. As such, it can be solved in a fast and effective fashion as a CP problem, and its intersection in turn results in a convex set in the space of the unknowns. Unfortunately, the same property does not hold true for the objective function (2), which is a non-convex form of the array excitations. Therefore, instead of directly performing (2), the optimal solution of the optimization problem (2), (3) can be effectively identified through the algorithm described by the flowchart of Fig. 3, i.e., once $M, N_C, z_1, \ldots, z_M$, θ_T, UB_Σ, UB_Δ, A_Σ, A_Δ, Ω_Σ, Ω_Δ, $f_{\max}$, and Δf have been chosen, repeatedly solve the CP problem (3) for increasing values of Q until constraints become so strict that no intersection exists anymore.

Notably, provided that the constraints admit a physical solution, the proposed design approach allows achieving, by definition, the configuration of the array excitations guaranteeing the maximum bandwidth.

Once the FBW is maximized, the user can perform further experiments in order to find additional optimal solutions. In fact, by keeping the array layout and fixing Q equal to the maximum possible value determined through the flowchart in Fig. 3, problem (3) can be solved for different values of N_C, UB_Σ, UB_Δ, A_Σ, A_Δ, Ω_Σ, and Ω_Δ in order to find the best trade-off between easiness of reconfiguration

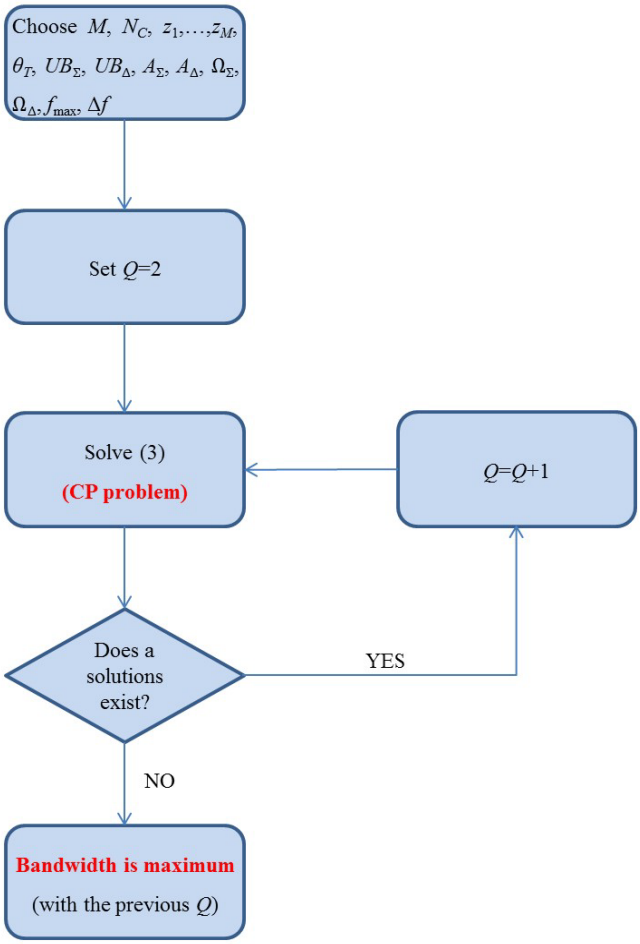

Figure 3. Flowchart of the developed synthesis algorithm. In case no feasible solutions exists for $Q = 2$, the user should relax the power-pattern masks or, alternatively, increase either M or N_C. Due to the very fast convergence of the algorithm guaranteed by the convex programming engine, the possible unfeasibility of the radiation constraints can be easily detected by the user. The user can even use the proposed approach to quickly ascertain whether or not the assigned power-pattern masks can be fulfilled by any particular array at hand or, alternatively, to identify the minimum number of array elements required to achieve a given radiation performance.

and radiation performances. In particular, for a given Q value, the larger the N_C is, the higher the expected radiation performance of the sum and difference patterns is. Conversely, the lower the N_C is, the lower the complexity of the BFN is (see above).

Summarizing, the advantages of the presented technique over the available methods can be summarized as follows:

- the maximization of the bandwidth is jointly performed, at the same time, for both the monopulse radiation modalities (while the available methods just maximize the bandwidth of one single beam);
- the adoption exclusively of convex programming algorithms ensures the maximization of performance as well as the minimization of the computational burden (while most of available methods recur to global optimization schemes such as evolutionary, ant colony, and simulated annealing algorithms which is way more complex and time-consuming and cannot afford the synthesis in the case of very large arrays);
- for the first time in the open literature concerned with monopulse arrays, the proposed method allows the user to maximize the bandwidth while a portion of the elements' excitations is shared between the two radiation modalities, which leads to a dramatic reduction of the beam forming network complexity.

The proposed method definitively improves the one introduced in [21]. In fact, while the latter is devoted to maximize the bandwidth of just one beam at a time, the new upgraded method allows simultaneously maximizing the bandwidth of the two beams requiring to the monopulse radar system. In particular, the new method allows the design of reconfigurable arrays whose excitations are optimized to boost the performance of both the sum and difference patterns.

Finally, it is worth noting that the proposed method is very general. In fact, it can be used for any kind of linear, planar, and conformal array working in either the far-field or the near-field regions and guaranteeing the bandwidth and SLL performance even in complex scenarios such as satellite [27] and concrete-embedded [28] telecommunications. This can be done by adding the active element patterns [15, 29] to the field computation (1).

3. NUMERICAL EXAMPLES

In order to validate the proposed approach, a set of selected examples taken from an extensive numerical analysis are reported in the following. All CP-based optimizations have been carried out by using the CVX software tool [30].

In the first example, a linear array of $N = 10$ elements, as considered in [7], with inter-element distance $d = 0.025\,\mathrm{m}$ is taken into account, and six elements (i.e., $N_C = 3$), three for each tail of the array, are assumed to have common amplitude coefficients for the sum and difference patterns. The mask of the sum pattern $UB_\Sigma(\theta)$ has been set to have a mainlobe beamwidth (BW) equal to 30° and an upper bound value in the sidelobe region Ω_Σ equal to $SLL = -31\,\mathrm{dB}$. Differently, the mask of the difference pattern $UB_\Delta(\theta)$ is defined by setting $BW = 52°$ and $SLL = -20\,\mathrm{dB}$.

Unlike [7] in which the sum and difference patterns were synthesized at a single frequency, the iterative CP-based procedure described in Section 2 has been used. In the optimization, $Q = 6$ frequency samples have been considered, and an array affording a sum pattern and a difference pattern fitting the mask constraints from the minimum frequency of $f_Q = f_{\min} = 6\,\mathrm{GHz}$ to the maximum frequency of $f_1 = f_{\max} = 8.9\,\mathrm{GHz}$ has been synthesized. The two sets of excitations obtained for the sum and difference patterns are reported in Table 1 where, for the sake of symmetry, only the excitations of half array are given. The power patterns of the optimized sum and difference modes for the $Q = 6$ frequencies are shown in Fig. 4 where it is possible to observe that the beam shapes completely satisfy the upper-bound mask constraints.

For each of the $Q = 6$ frequency samples, the peak sidelobe level of both the sum (say SLL^Σ) and difference (say SLL^Δ) patterns, the peak directivity of the sum pattern (say $D^\Sigma_{\max}$), and the slope of the difference pattern (say K) have been computed and are reported in Table 2. As expected, it turns out that the sum pattern with the maximum directivity is obtained at $f_1 = f_{\max}$ and the minimum one at $f_Q = f_{\min}$, having a value equal to 11.14 dBi and 9.22 dBi (Table 2), respectively. As for the

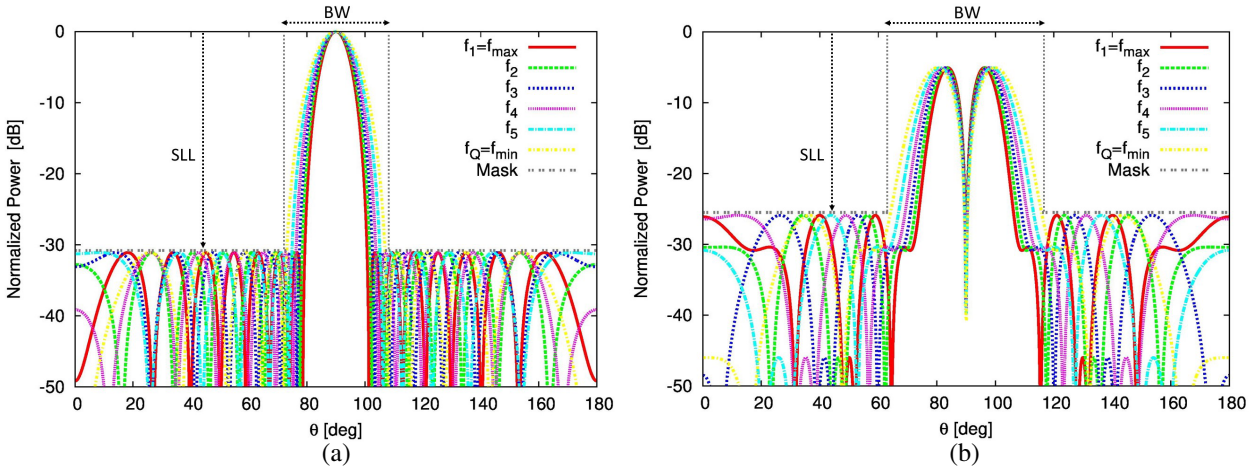

Figure 4. (a) Sum and (b) difference power patterns generated by the array antenna at $Q = 6$ frequency samples for the case $N = 10$ and $N_C = 3$ together with the mask constraints.

Table 1. CP-optimized amplitude coefficients for $N = 10$ and $N_C = 3$.

m	a_m^{Σ}	a_m^{Δ}	$z_m[\times 10^{-2}]$ [m]
1	1.000	0.252	1.25
2	0.874	0.716	3.75
3	0.658	0.658	6.25
4	0.415	0.415	8.75
5	0.236	0.236	11.25

Table 2. Patterns parameters for $N = 10$ and $N_C = 3$.

f	$d_f[\lambda_f]$	SLL^{Σ} [dB]	SLL^{Δ} [dB]	$D_{\max}^{\Sigma}$ [dBi]	K [1/rad]
$f_1 = f_{\max} = 8.90$ [GHz]	0.733	−31.09	−20.82	11.14	1.04
$f_2 = 8.32$ [GHz]	0.693	−31.09	−20.82	10.82	1.01
$f_3 = 7.74$ [GHz]	0.645	−31.09	−20.82	10.47	0.98
$f_4 = 7.16$ [GHz]	0.597	−31.09	−20.82	10.10	0.94
$f_5 = 6.58$ [GHz]	0.548	−31.09	−20.82	9.68	0.90
$f_Q = f_{\min} = 6.00$ [GHz]	0.500	−31.09	−20.82	9.22	0.85

boresight slope of the difference pattern, the highest value is achieved at $f_1 = f_{\max}$ (i.e., 1.04 [1/rad]) and the smallest at $f_Q = f_{\min}$ (i.e., 0.85 [1/rad]), respectively.

In the second example, two arrays having $N = 10$ and $N = 20$ elements with the same inter-element distance of the first example (i.e., $d = 0.025\,\mathrm{m}$) are considered. The percentage of elements having common amplitudes has been varied from 40% (i.e., $N_C = \{4, 8\}$ for $N = \{10, 20\}$) up to 80% (i.e., $N_C = \{2, 4\}$ for $N = \{10, 20\}$) to assess the array performance achievable by means of the proposed method when varying the number of degrees of freedom (DoFs) of the synthesis. In the optimization, the same upper-mask constraints of the first example have been taken into account for both the sum and the difference patterns.

Table 3. SLL of the sum and difference patterns and array FBW when $N = 10$ and $N_C = \{2, 3, 4\}$.

N_C	SLL^{Σ} [dB]	SLL^{Δ} [dB]	FBW
4	−31.03	−20.80	0.462
3	−31.09	−20.82	0.437
2	−31.18	−20.40	0.295

Table 4. SLL of the sum and difference patterns and array FBW when $N = 20$ and $N_C = \{4, 6, 8\}$.

N_C	SLL^{Σ} [dB]	SLL^{Δ} [dB]	FBW
8	−31.75	−21.44	0.672
6	−31.96	−21.28	0.647
4	−31.00	−20.36	0.479

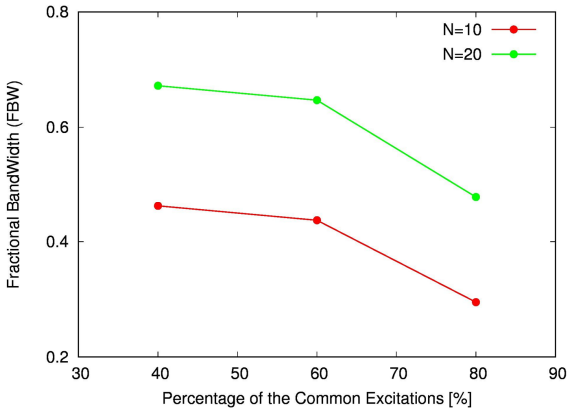

Figure 5. FBW of the designed array antennas versus the number of common amplitude coefficients.

It is possible to observe that in all cases the mask requirements are satisfied as noticeable from the *SLL* values in Table 3 and Table 4 for the array having $N = 10$ and $N = 20$ elements, respectively. Moreover, the values of the FBW for the CP-based synthesized solutions are reported in Fig. 4. It is evident that the more the DoFs is available in the design, the larger the operation bandwidth is achieved for the synthesized array antennas. More specifically, the FBW of the smaller array having $N = 10$ elements varies from a maximum of $FBW = 0.462$ when $N_C = 4$ to a minimum of $FBW = 0.295$ when $N_C = 2$ (Table 3) thus showing wideband performances (i.e., $0.2 < FBW < 0.5$). On the other hand, larger FBWs are obtained with the array having $N = 20$ elements, with $FBW = 0.672$ and $FBW = 0.647$ when $N_C = 8$ and $N_C = 6$, respectively, in this case demonstrating an ultra-wideband behavior (i.e., $FBW > 0.5$). All these results are summarized in Fig. 5, which shows the achieved FBW as a function of the percentage of the shared excitations between the sum and difference radiation modalities.

In the third and last example, in order to evaluate the effectiveness and versatility of the proposed method in synthesizing sum and difference patterns with arbitrary upper-bound masks, let us consider an array having $N = 20$, $d = 0.025\,\mathrm{m}$, and $N_C = 6$. To highlight the capability of the proposed technique to allow enforcing completely-arbitrary power masks, the upper-bound constraints have been this time set in such a way to induce two notches (i.e., sidelobe suppressions) centered at $\theta = 53°$ and $\theta = 127°$ having the depth and width of 20 dB and 14°, respectively, as shown in Fig. 6. The mainlobe beamwidth and sidelobe level of the masks for the sum and difference patterns have been set

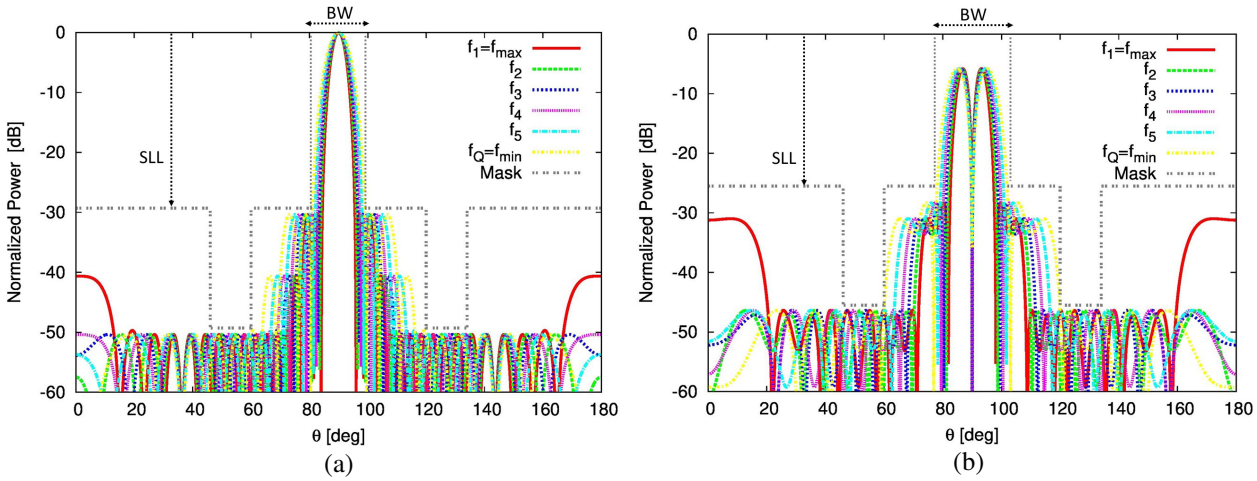

Figure 6. (a) Sum and (b) difference power patterns generated by the array antenna at $Q = 6$ frequency samples for the case $N = 20$ and $N_C = 6$ together with the mask constraints.

to ($BW = 18°$, $SLL = -31\,\text{dB}$) and ($BW = 24°$, $SLL = -25\,\text{dB}$), respectively. The power patterns of the synthesized sum and difference beams are shown in Fig. 6. It is possible to observe that the mask constraints are completely satisfied thanks to the CP-based method. Moreover, wideband antenna performances are provided since $FBW = 0.387$.

4. CONCLUSIONS

In this work, an innovative method for the optimal synthesis of wideband array antennas for monopulse radar applications guaranteeing the maximum operation bandwidth given the array geometry and upper-bound power masks on the sum and difference patterns has been proposed. The method has also allowed significantly reducing the complexity of the beam forming network thanks to the possibility to enforce common-excitation amplitudes for the elements located in the tail of the arrays

The capability of designing wideband as well as ultra-wideband array antennas with different trade-offs in terms of complexity of the user-defined mask constraints and number of common-amplitude coefficients has been demonstrated through a large set numerical examples. The optimality of the achieved results and the minimization of the computational burden have been ensured thanks to the formulation of the synthesis problem as a sequence of CP optimizations.

ACKNOWLEDGMENT

This work was supported in part by the Italian Ministry of University and Research under the PRIN research project "CYBER-PHYSICAL ELECTROMAGNETIC VISION: Context-Aware Electromagnetic Sensing and Smart Reaction", prot. 2017HZJXSZ.

REFERENCES

1. Ren, Y., J. Wang, D. C. Hu, and N. Zhang, "Horn-based circular polarized antenna array with a compact feeding for Ka-band monopulse antenna," *Progress In Electromagnetics Research*, Vol. 142, 291–308, 2013.
2. Oliveri, G. and L. Poli, "Synthesis of monopulse sub-arrayed linear and planar array antennas with optimized sidelobes," *Progress In Electromagnetics Research*, Vol. 99, 109–129, 2009.
3. Morabito, A. F. and P. Rocca, "Reducing the number of elements in phase-only reconfigurable arrays generating sum and difference patterns," *IEEE Antennas and Wireless Propagation Letters*, Vol. 14, 1338–1341, 2015.

4. Ares, F., J. A. Rodriguez, E. Moreno, and S. R. Rengarajan, "Optimal compromise among sum and difference patterns," *Journal of Electromagnetic Waves and Applications*, Vol. 10, No. 11, 1543–1555, 1996.
5. Caorsi, S., A. Massa, M. Pastorino, and A. Randazzo, "Optimization of the difference patterns for monopulse antennas by a hybrid real/integer coded differential evolution method," *IEEE Transactions on Antennas and Propagation*, Vol. 53, No. 1, 372–376, 2005.
6. Manica, L., P. Rocca, M. Benedetti, and A. Massa, "A fast graph-searching algorithm enabling the efficient synthesis of sub-arrayed planar monopulse antennas," *IEEE Transactions on Antennas and Propagation*, Vol. 57, No. 3, 652–663, Mar. 2009.
7. Morabito, A. F. and P. Rocca, "Optimal synthesis of sum and difference patterns with arbitrary sidelobes subject to common excitations constraints," *IEEE Antennas and Wireless Propagation Letters*, Vol. 9, 623–626, 2010.
8. Rocca, P. and A. F. Morabito, "Optimal synthesis of reconfigurable planar arrays with simplified architectures for monopulse radar applications," *IEEE Transactions on Antennas and Propagation*, Vol. 63, No. 3, 1048–1058, 2015.
9. Morabito, A. F., A. R. Lagana, and T. Isernia, "Optimizing power transmission in given target areas in the presence of protection requirements," *IEEE Antennas and Wireless Propagation Letters*, Vol. 14, 44–47, 2015.
10. Leonardi, O., M. G. Pavone, G. Sorbello, A. F. Morabito, and T. Isernia, "Compact single-layer circularly polarized antenna for short-range communication systems," *Microwave and Optical Technology Letters*, Vol. 56, No. 8, 1843–1846, 2014.
11. Palmeri, R., M. T. Bevacqua, A. F. Morabito, and T. Isernia, "Design of artificial-material-based antennas using inverse scattering techniques," *IEEE Transactions on Antennas and Propagation*, Vol. 66, No. 12, 7076–7090, 2018.
12. Battaglia, G. M., A. F. Morabito, R. Palmeri, and T. Isernia, "Constrained focusing of vector fields intensity in near zone and/or complex scenarios as a low-dimensional global optimization," *Journal of Electromagnetic Waves and Applications*, Vol. 34, No. 15, 1977–1989, 2020.
13. Battaglia, G. M., G. G. Bellizzi, A. F. Morabito, G. Sorbello, and T. Isernia, "A general effective approach to the synthesis of shaped beams for arbitrary fixed-geometry arrays," *Journal of Electromagnetic Waves and Applications*, Vol. 33, No. 18, 2404–2422, 2019
14. Morabito, A. F., R. Palmeri, V. A. Morabito, A. R. Laganà, and T. Isernia, "Single-surface phaseless characterization of antennas via hierarchically ordered optimizations," *IEEE Transactions on Antennas and Propagation*, Vol. 67, No. 1, 461–474, 2019.
15. Morabito, A. F., A. Di Carlo, L. Di Donato, T. Isernia, and G. Sorbello, "Extending spectral factorization to array pattern synthesis including sparseness, mutual coupling, and mounting-platform effects," *IEEE Transactions on Antennas and Propagation*, Vol. 67, No. 7, 4548–4559, 2019.
16. Nikkhah, M. R., M. Hiranandani, and A. A. Kishk, "Rotman lens design with wideband DRA array," *Progress In Electromagnetics Research*, Vol. 169, 45–57, 2020.
17. Chen, Y., S. Yang, and Z. P. Nie, "A novel wideband antenna array with tightly coupled octagonal ring elements," *Progress In Electromagnetics Research*, Vol. 124, 55–70, 2012.
18. Lee, W. S., K. S. Oh, and J. W. Yu, "A wideband planar monopole antenna array with circular polarized and band-notched characteristics," *Progress In Electromagnetics Research*, Vol. 128, 381–398, 2012.
19. Liu, P., Y. Sun, T. Liu, Q. Li, and X. Wang, "Wideband 10-port MIMO antenna array for 5G metal-frame smartphone applications," *Progress In Electromagnetics Research C*, Vol. 104, 229–240, 2020.
20. Zheng, Y., M. Gao, and X. Zhao, "A novel patch array antenna with wideband and dual sense circular polarization characteristics for WiMAX & WLAN applications," *Progress In Electromagnetics Research C*, Vol. 99, 123–132, 2020.

21. Bui, L. T. P., N. Anselmi, T. Isernia, P. Rocca, and A. F. Morabito, "On bandwidth maximization of fixed-geometry arrays through convex programming," *Journal of Electromagnetic Waves and Applications*, Vol. 34, No. 5, 581–600, 2020.
22. Isernia, T. and G. Panariello, "Optimal focusing of scalar fields subject to arbitrary upper bounds," *Electronics Letters*, Vol. 34, No. 2, 162–164, 1998.
23. Bucci, O. M., C. Gennarelli, and C. Savarese, "Representation of electromagnetic fields over arbitrary surfaces by a finite and nonredundant number of samples," *IEEE Transactions on Antennas and Propagation*, Vol. 46, No. 3, 351–359, 1998.
24. Capek, M., L. Jelinek, and P. Hazdra, "On the functional relation between quality factor and fractional bandwidth," *IEEE Transactions on Antennas and Propagation*, Vol. 63, No. 6, 2787–2790, 2015.
25. Allen, B., T. Brown, K. Schwieger, E. Zimmermann, W. Q. Malik, D. J. Edwards, L. Ouvry, and I. Oppermann, "Ultrawideband: Applications, technology and future perspectives," *Proceedings of the International Workshop on Convergent Technologies (IWCT)*, Oulu, Finland, Jun. 6–10, 2005.
26. Bevelacqua, P. J. and C. A. Balanis, "Geometry and weight optimization for minimizing sidelobes in wideband planar arrays," *IEEE Transactions on Antennas and Propagation*, Vol. 57, No. 4, 1285–1289, 2009.
27. Morabito, A. F., A. R. Laganà, and L. Di Donato, "Satellite multibeam coverage of earth: Innovative solutions and optimal synthesis of aperture fields," *Progress In Electromagnetics Research*, Vol. 156, 135–144, 2016.
28. Mauro, G. S., G. Castorina, A. F. Morabito, L. Di Donato, and G. Sorbello, "Effects of lossy background and rebars on antennas embedded in concrete structures," *Microwave and Optical Technology Letters*, Vol. 58, 2653–2656, 2016.
29. Battaglia, G. M., A. F. Morabito, G. Sorbello, and T. Isernia, "Mask-constrained power synthesis of large and arbitrary arrays as a few-samples global optimization," *Progress In Electromagnetics Research C*, Vol. 98, 69–81, 2020.
30. CVX Research, Inc., "CVX: Matlab software for discipline convex programming," Version 2.0 Beta, Sep. 2012, http://cvxr.com/cvx.